Fabry-Perot Interferometer FABRYPEROT.TEX KB 20020122

KLAUS BETZLER[1], FACHBEREICH PHYSIK, UNIVERSITÄT OSNABRÜCK

This short lecture note recalls some of the properties of Fabry-Perot interferometers. As an addition to textbooks, it may present some help to students working with such instruments. It is neither intended as a substitute for textbooks in optics nor as a comprehensive overview over the field of Fabry-Perot interferometers.

1 Principles of the Fabry-Perot Interferometer

The Fabry-Perot interferometer is an optical instrument which uses *multiple-beam interference*. Its transfer function is that of a plane-parallel plate which is described in textbooks for optics [1].

1.1 Interference at a Plane-Parallel Plate

First we calculate the transmitted and reflected intensity when shining a plane wave of monochromatic light on a plane-parallel plate.
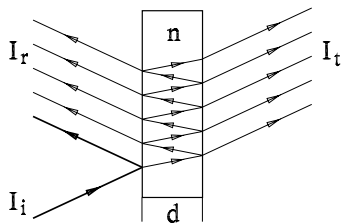

Figure 1: Interference at a plane-parallel plate of thickness d.

The situation is depicted in Fig. 1, light of intensity I_i, wavelength λ and wavevector $k = 2\pi/\lambda$ is incident on a plate of thickness d and refractive index n. The two surfaces affected may both be characterized by a reflectance R and a transmittance T, defined for the light *intensities*. The absorption of the plate material should be negligible, thus $R + T = 1$ (energy conservation).

To calculate the transmitted and reflected intensities I_t and I_r, we have to sum up the amplitudes of the respective waves, taking into account the phase shifts imposed by the plate. Reflectance and transmittance for the *amplitudes* at the plate interfaces, r, r', t, and t', respectively, are defined according to Fig. 2.

Relations between the reflectance and transmittance values for amplitudes can be derived using time reversal invariance. If losses due to absorption can be neglected,
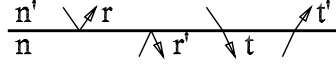
---

[1] KLAUS.BETZLER@UOS.DE

Figure 2: Definition of reflectance and transmittance at an interface between two non-absorbing materials.

the propagation of waves must be reversible. Fig. 3 shows the 'normal' and the reversed beam propagation through a surface and denotes the corresponding amplitudes.
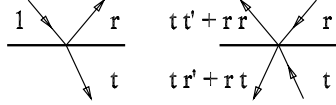

Figure 3: 'Normal' (left) and time reversed (right) reflection and transmission at an interface.

A comparison yields

$$tt' + rr = 1 \tag{1}$$

$$tr' + rt = 0 \quad . \tag{2}$$

Therefore

$$r' = -r \quad , \quad r'^2 = r^2 = R \quad , \quad tt' = T = 1 - R \quad . \tag{3}$$

Fig. 1, to yield a descriptive visualization, is sketched with oblique incidence of the light – the derivation of the transfer function, yet, will be done using normal incidence.

The reflected amplitude is calculated by summing all reflected waves. Different waves m differ in phase due to the optical path difference $2mdn$ and in amplitude due to reflection and transmission by $tt' \cdot r'^{2m-1}$. The first reflected wave has to be considered with special care, here the reflectance for the 'out-in' direction $- r -$ has to be used. Putting all together, we get for the reflected amplitude

$$
\begin{aligned}
A_r &= A_i r + A_i \exp(jk2dn) tt' r' \sum_{m=0}^{\infty} r'^{2m} \exp(jk2mdn) \tag{4} \\
&= A_i r - A_i \exp(j\delta) T r \sum_{m=0}^{\infty} \left(R \exp(j\delta) \right)^m, \quad \delta = 2kdn \tag{5} \\
&= A_i r - A_i \exp(j\delta) T r \frac{1}{1 - R \exp(j\delta)} \tag{6} \\
&= A_i r \frac{1 - R \exp(j\delta) - T \exp(j\delta)}{1 - R \exp(j\delta)} = A_i r \frac{1 - \exp(j\delta)}{1 - R \exp(j\delta)} \tag{7}
\end{aligned}
$$

and for the intensity

$$I_r = A_r \cdot A_r^* \tag{8}$$

which – after some conversions – yields

$$\frac{I_r}{I_i} = \frac{2R(1 - \cos\delta)}{1 - 2R\cos\delta + R^2} = \frac{4R\sin^2\frac{\delta}{2}}{(1 - R)^2 + 4R\sin^2\frac{\delta}{2}} \quad . \tag{9}$$

For the transmitted amplitude the expression gets a little bit simpler

$$A_t = A_i t t' \sum_{m=0}^{\infty} r'^{2m} \exp(jk2mdn) \tag{10}$$

$$= A_i T \sum_{m=0}^{\infty} R^m \exp(j\delta) \tag{11}$$

$$= A_i \frac{T}{1 + R\exp(j\delta)} \tag{12}$$

and

$$\frac{I_t}{I_i} = \frac{T^2}{1 - 2R\cos\delta + R^2} = \frac{T^2}{(1 - R)^2 + 4R\sin^2\frac{\delta}{2}} \quad . \tag{13}$$

Eq. 13 of course also may be obtained directly from Eq. 9 using $I_r + I_t = I_i$ (energy conservation law). The expressions for the reflected and transmitted intesities Eqs. 9 and 13 are known as *Airy*'s formula.

One can define a quality factor for the reflectivity

$$Q_R = \frac{4R}{(1 - R)^2} \tag{14}$$

which simplifies the expressions Eqs. 9 and 13 further

$$\frac{I_r}{I_i} = \frac{Q_R\sin^2\frac{\delta}{2}}{1 + Q_R\sin^2\frac{\delta}{2}} \tag{15}$$

$$\frac{I_t}{I_i} = \frac{1}{1 + Q_R\sin^2\frac{\delta}{2}} \quad . \tag{16}$$

This quality factor Q_R sometimes is denoted as *finesse coefficient* (see section 1.4 f.).

It should be noted that at the transmission peaks all of the incident intensity is transmitted, nothing reflected, even when using highly reflecting surfaces.

Fig. 4 shows a plot of the transmittance function Eq. 16 for different values of Q_R. Instead of δ, the corresponding interference order $N = \delta/2\pi$ is noted.

Two properties are characteristic for each of the transmission functions, the width of the maxima and the suppression of light throughput between the maxima.
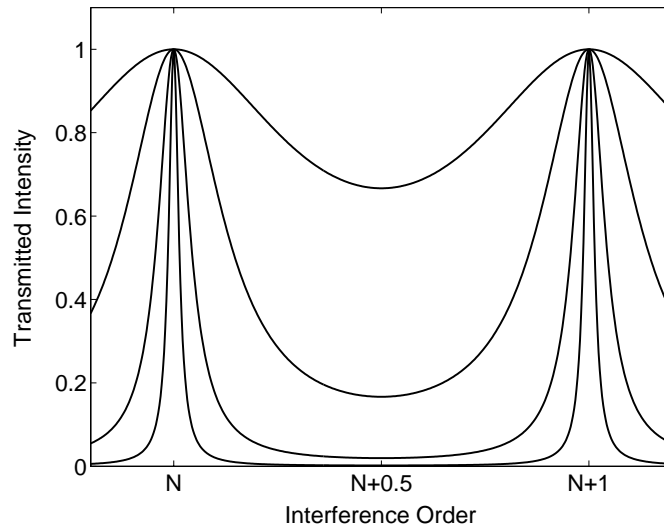
Figure 4: The transfer function I_t/I_i of a plane-parallel plate (Fabry-Perot plate) for different reflectivities (quality factors 0.5, 5, 50, and 500, respectively, corresponding to reflectivities R of 0.1, 0.42, 0.75, 0.91).

1.2 Applications

The transfer function shows high transmission when certain conditions for the wavelength of the light and the plate geometry are fulfilled, otherwise the light is more or less blocked. These conditions can be adjusted by changing the wavelength and/or the geometry. Thus Fabry-Perot plates can be used to measure or to control light wavelengths or to measure geometric properties. The geometric conditions are defined by several properties including thickness, refractive index, and beam direction. As a Fabry-Perot arrangement is very sensitive with regard to the geometry, small deviations in these properties can be measured. The same sensitivity facilitates various optical applications. A Fabry-Perot plate, e. g., can be used in a laser resonator to select single longitudinal modes, the adjustment is made by tilting it with respect to the beam direction.

Very important is the application for high-resolution optical spectroscopy. To use a Fabry-Perot interferometer there, one of the geometric properties has to be adjustable and to be related in a suitable way to wavelength variations. With plates, this can be achieved when using divergent light, thus different beam directions. More customary are air-spaced interferometers, where spacing or air-pressure are used for tuning.

1.3 Fringes of Equal Inclination

Using – as shown in Fig. 5 – as light source for a Fabry-Perot plate either an extended light source in the focal plane of a collimating lens or a divergent point source produces concentric circular interference fringes due to the inclination-dependent phase shifts (fringes of equal inclination).
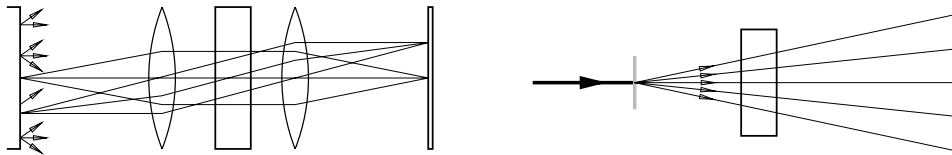

Figure 5: Experimental arrangements for fringes of equal inclination. Left: extended source in the focal plane of the collimating lens, right: divergent point source.

Typical fringe patterns for monochromatic light sources (calculated for plates of different reflectivity) are shown in Fig. 6.
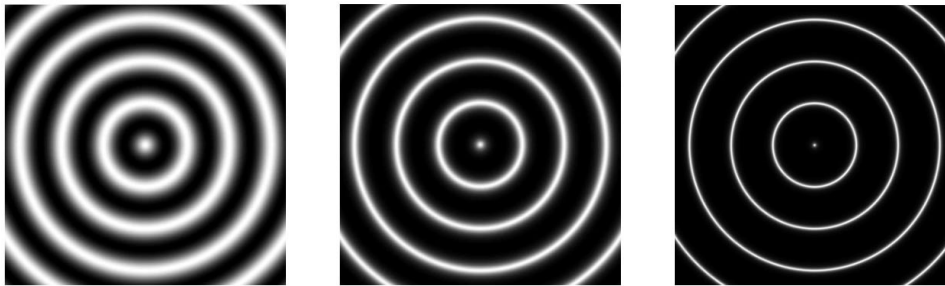

Figure 6: Fringes of equal inclination for Fabry-Perot plates of different reflectivity. From left to right: finesse coefficients = 1, 10, 100.

Arrangements like that on the right of Fig. 5 – a diffusor plate in combination with a Fabry-Perot plate – can be used as a simple means to check linewidth and mode structure of lasers.

1.4 Finesse

It is costumary to define a numerical value which characterizes the width – or better the sharpness – of the maxima. This number is called *Finesse* of an interferometer and defined as the ratio of peak distance to peak halfwidth.

To get it, the points (phases δ) where the transfer function reaches a value of 0.5 have to be calculated

$$\frac{1}{1 + Q_R \sin^2 \frac{\delta}{2}} \overset{!}{=} 0.5 \quad , \tag{17}$$

$$Q_R \sin^2 \frac{\delta}{2} = 1 \quad \text{and for } |\delta - 2N\pi| \ll 1 : \quad \delta = \pm \frac{2}{\sqrt{Q_R}} \quad . \tag{18}$$

The distance (phase difference) between two peaks is 2π, thus the Finesse F is

$$F = \frac{\pi}{2}\sqrt{Q_R} = \frac{\pi\sqrt{R}}{1-R} \quad . \tag{19}$$

As only the influence of the reflectivity on the linewidth is considered here, often the term *Reflectivity Finesse* is used to distinguish it from other properties influencing the transfer function (divergence – see Sec. 2.3, plate flatness – see Sec. 2.4).

1.5   Contrast

To rate the suppression between maxima, the *Contrast* is defined as ratio of peak height to the minimum intensity. The transmission minimum at $\delta = \pi$ and at equivalent phases define a Contrast value C of

$$C = Q_R + 1 \quad . \tag{20}$$

1.6   Resolution

The resolution of an optical instrument is defined by the bandwidth of a spectral line, i. e. the broadening imposed on the line by the instrument. We have to calculate what spectral linewidth $\Delta\lambda$ is equivalent to this instrumental linewidth. As hitherto, we assume normal incidence. At the maxima, the phase difference δ is defined by

$$\delta = 2kdn = \frac{4\pi}{\lambda}dn = 2N\pi \quad . \tag{21}$$

The linewidth can be expressed by the finesse

$$\Delta\delta = \frac{2\pi}{F} \quad , \tag{22}$$

and equated with a spectral linewidth

$$\Delta\delta = \frac{2\pi}{F} = \frac{4\pi}{\lambda}dn - \frac{4\pi}{\lambda + \Delta\lambda}dn \quad . \tag{23}$$

Thus the resolving power of the instrument is defined by the product of the finesse F and the interference order N

$$\frac{\lambda}{\Delta\lambda} = \frac{2F}{\lambda}dn = F \cdot N \quad . \tag{24}$$

Eq. 24 shows that, with a finesse of 100, the resolving power of a 100 mm wide grating is exceeded for $dn > 0.5$ mm. Using air-spaced Fabry-Perot interferometers, values for d up to more than 100 mm can be easily achieved. The resolution then – expressed as frequency – is around 10 MHz.

1.7 Free Spectral Range

Taking Eq. 24, the resolution of a Fabry-Perot plate can be improved by increasing dn, the optical path difference between the two reflecting surfaces. But, doing this, also the interference order is increased, leading to more problems with overlapping orders. As a measure for the useful working range (no overlapping orders) the *Free Spectral Range* of an instrument is defined. It is calculated by equating the phase shift for a certain wavelength λ, order $N + 1$ with that for $\lambda + \mathrm{FSR}$, order N:

$$\frac{2dn}{\lambda} = \frac{2dn}{\lambda + FSR} + 1 \tag{25}$$

$$\mathrm{FSR} = \Delta\lambda_{\mathrm{FSR}} = \frac{\lambda^2}{2dn} \quad . \tag{26}$$

Compared to the resolution

$$\frac{\Delta\lambda_{\mathrm{FSR}}}{\Delta\lambda_{\mathrm{res}}} = F \quad . \tag{27}$$

2 Tunable Fabry-Perot Interferometers

Parallel-plate Fabry-Perot interferometers, often denoted as *Etalons*, can be tuned by inclining them with respect to the beam direction, thus varying the phase shift inside the plate. This principle is used, e. g., to select single modes inside a laser resonator. For spectroscopic applications, yet, different schemes have to be applied.

2.1 The Air-Spaced Fabry-Perot Interferometer

Nearly all tuning schemes use interferometers where two highly reflective glass plates are separated by a plane-parallel 'plate' of air. The scheme is complementary to the plane-parallel plate discussed and obeys the same equations.

Fig. 7 shows the principle, the two plates usually are slightly wedge-shaped to suppress interference due to the outer surfaces. As the optical distance between the
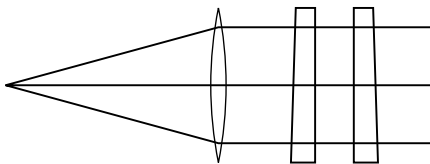

Figure 7: Air-spaced Fabry-Perot interferometer. Parallel light is achieved using a point source in the focus of the illuminating lens.

two plates is $d \cdot n$, a convenient way to change it is to vary the air pressure. That was classically used, keeping the distance d constant by mechanical spacers and varying the refractive index n of the air by changing the pressure. Nowadays, this technique is – at best – only of historical interest.

2.2   The Scanning Fabry-Perot Interferometer

The preferred method used for scanning is to move one of the two reflecting plates mechanically. The principle is shown in Fig. 8. As the mechanical scanning distance necessary is in the order of the light wavelength this scanning can be done by piezoelectric actuators.
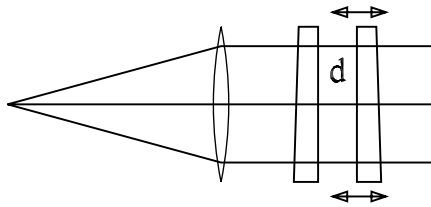

Figure 8: Scanning Fabry-Perot interferometer, principle. The space d between the two reflecting surfaces is varied by moving on of the plates.

The actuators can be driven at moderate voltages $(100 \ldots 500$ V), to get linear scans, usually sawtooth waveforms are used.

Piezoelectric scanning has a variety of advantages compared to other scanning techniques:

- Both, slow and fast scanning modes are possible. In fast scanning modes, the interferogram may be displayed online on an oscilloscope.

- The scanning voltage can be directly used as measure for the plate position.

- The final adjustment can be easily done by automatically or manually adjusting the drive voltages of the (usually three) piezo stacks.

- Stabilization schemes can be easily included by controlling the drive voltages of the piezo stacks. The controller, e. g., can try to hold a constant position and height of the peaks [2, 3].

There is also one disadvantage of piezoelectric actuators, they often show a large temperature drift, thus they have to be driven in controlled mode.

2.3   Pinhole, Divergence

So far we have considered the ideal case of an exact plane wave or exactly parallel light beams. One can construct this ideal case using a point source in the focus of an illuminating lens (Fig. 8). In a real-world system, yet, one always has to deal with extended light sources. To approach the ideal case, pinholes are used as an approximation to a point source. The light throughput of the instrument is proportional to the pinhole area, but, increasing the pinhole size, also increases the divergence of the light in the instrument. Thus, to maximize the efficiency, the pinhole size has to be optimized.
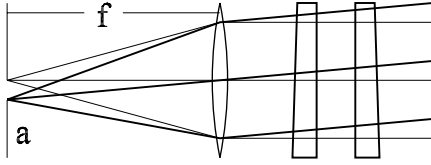
Figure 9: Divergence imposed by a pinhole of radius a.

From Fig. 9, the angle between central and outermost beams can be derived to be

$$\alpha = \arcsin \frac{a}{f} \approx \frac{a}{f} \quad . \tag{28}$$

This results in a corresponding path difference

$$\Delta d = d(\frac{1}{\cos \alpha} - 1) \approx d\frac{\alpha^2}{2} \approx d\frac{a^2}{2f^2} \quad , \tag{29}$$

which will impose an additional phase shift and thus broaden the peaks in the interferogram. To keep a good resolution, the additional broadening due to this path difference should be less than the halfwidth of the peaks

$$\Delta\delta_{\mathrm{pinhole}} < \Delta\delta_{\mathrm{linewidth}} \quad , \tag{30}$$

using Eqs. 22 and 29

$$2k\Delta d = \frac{2\pi}{\lambda}d\frac{a^2}{f^2} < \frac{2\pi}{F} \quad , \tag{31}$$

for the pinhole radius

$$a < f\sqrt{\frac{\lambda}{Fd}} \quad . \tag{32}$$

For typical geometry data – $d = 5$ mm, $f = 200$ mm, $\lambda = 0.5\ \mu$m, $F = 100$ – this results in a radius $a < 200\ \mu$m.

The influence of the pinhole on the linewidth of a Fabry-Perot interferometer can be denoted as *Pinhole Finesse* which is defined as

$$F_{\mathrm{P}} = \frac{\lambda}{d} \cdot \frac{f^2}{a^2} \quad . \tag{33}$$

2.4 Plate Flatness

Due to the multiple reflections in a Fabry-Perot interferometer, deviations in the homogeneity of the reflecting surfaces are 'multiplied', too.

3 Enhancements to the Fabry-Perot Interferometer

As has been shown in the previous sections, the Fabry-Perot interferometer combines excellent resolution with a rather poor free spectral range and, moreover,

a low contrast which doesn't allow measurements of spectra with high intensity differences. To overcome these drawbacks, several enhancements have been introduced.

3.1 Combination with a Spectrometer

A classical setup is the combination of a Fabry-Perot plate with a spectrometer as shown in Fig. 10. The spectrometer provides for gross resolution, the Fabry-Perot interferometer allows for the determination of spectral linewidths or line splittings. As light source a slit perpendicular to the drawing plane of Fig. 10 is used. Thus, for each of the lines in such a spectrum, partial fringes of equal inclination are produced which can be evaluated. Examples for such spectra can be found in textbooks on optics [1].
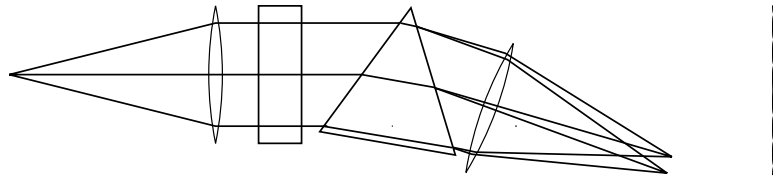
Figure 10: Combination of a Fabry-Perot plate with a conventional prism spectrometer. As light source on the left a slit is used. Thus a gross spectral resolution in the drawing plane due to the prism is achieved. Perpendicular to the drawing plane, partial fringes of equal inclination are generated – as shown on the right – which allow for an evaluation of finer structures.

3.2 Multipass

To enhance the contrast of a Fabry-Perot interferometer, it can be used more than once. The principle of such a *multipass* scheme for three passes is shown in Fig.11. A narrower light beam is used which – using appropriate retroreflectors – is directed three times through the instrument.
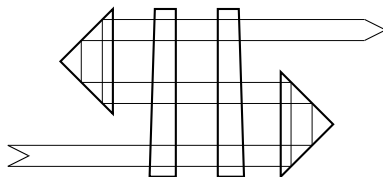
Figure 11: Principle of a multipass interferometer. The light passes three times through the interferometer.

Figs. 12 (linear scale) and 13 (logarithmic scale) show the enhancements in contrast due to the multipass scheme.
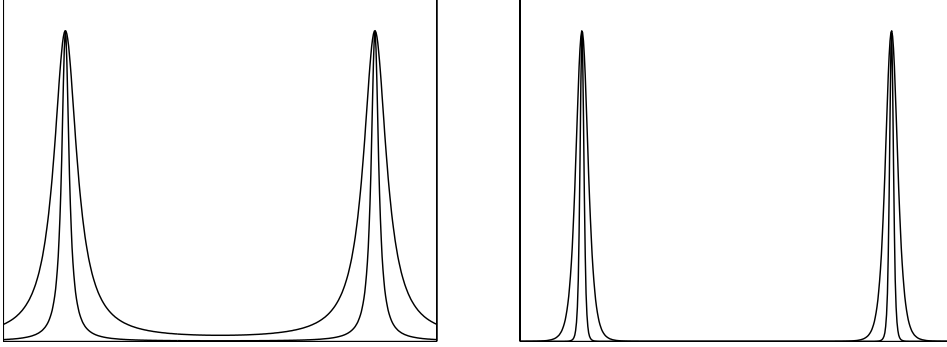
Figure 12: Comparison of the transfer functions between a single pass (left) and a triple pass interferometer (right) for two different finesse coefficients (50 and 500).
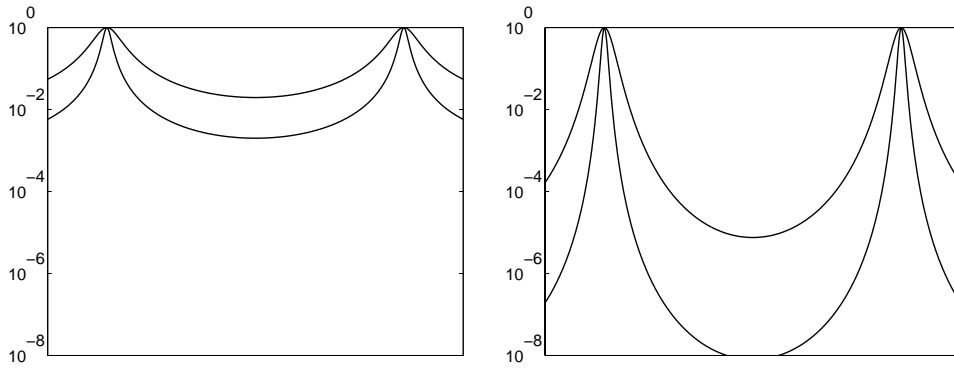

Figure 13: As Fig. 12, but with logarithmic scaling.

3.3 Tandem

To overcome the free-spectral-range problem, a similar approach as that already discussed uses two different interferometers with different spectral ranges in conjunction, one for coarse, one for finer resolution.

The two interferometers work in different interference orders N_1 and N_2 respectively. They have to be synchronized such that in the spectral region investigated the interference maxima for all wavelengths coincide:

$$\lambda \;=\; \frac{2(dn)_1}{N_1} = \frac{2(dn)_2}{N_2} \tag{34}$$

$$\lambda + \Delta\lambda \;=\; \frac{2((dn)_1 + \Delta(dn)_1)}{N_1} = \frac{2((dn)_2 + \Delta(dn)_2)}{N_2} \quad . \tag{35}$$

Eq. 35 also ensures that

$$\frac{2((dn)_1 + \Delta(dn)_1)}{N_1 + 1} \neq \frac{2((dn)_2 + \Delta(dn)_2)}{N_2 + 1} \quad \text{for} \quad N_1 \neq N_2 \quad , \tag{36}$$

thus neighboring orders are suppressed.

The synchronization condition defined by Eqs. 34 and 35 necessitates that – besides a synchronization at λ – also the tuning of the two interferometers has to be synchronized according to

$$\Delta(dn)_1 : \Delta(dn)_2 = (dn)_1 : (dn)_2 \quad . \tag{37}$$

One way to achieve this is to use air spaced interferometers with fixed spacing which are tuned by the air pressure in a common compartment. Equal Δn values in both systems obviously fulfill the above condition.

A different, very elaborate technique is used in the interferometers build by J. R. Sandercock [4]. The principle scheme is sketched in Fig. 14: The two interferometers are tilted against each other by an angle α, the adjustment is made such that the ratio between the two spacings obeys the condition

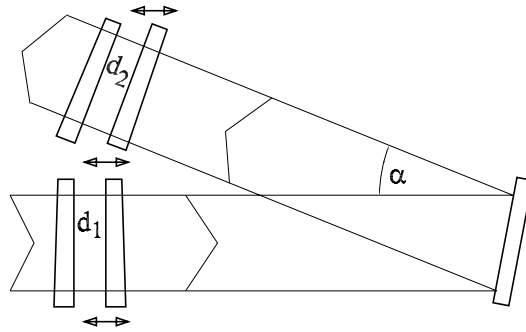$$d_2 : d_1 = \cos \alpha \quad . \tag{38}$$

Figure 14: Tandem interferometer with mechanical coupling of the two movable plates. The double arrows indicate the direction of movement.

When tuning, the movements of the two movable plates are coupled using joint mechanics; the direction of the movement is indicated in Fig. 14. Through this mechanical setup it is ensured that

$$\Delta d_2 : \Delta d_1 = \cos \alpha \tag{39}$$

which – combined with Eq. 38 – directly fulfills the synchronization condition Eq. 37.

The following figures show calculated examples for interferograms measured with a tandem interferometer. The interference orders of the two interferometers are $N_1 = 1000$ and $N_2 = 1100$, respectively.

Fig. 15 shows the interferograms for a single monochromatic spectral line, Fig. 16 for two adjacent lines. The upper two interferograms are measured with each of the individual interferometers, the lower shows the effect of the tandem combination.

An expressed effect is the drastically increased free spectral range. But, as can be also stated from the figures, due to the poor contrast of an interferometer, the neighboring orders are not fully suppressed. Instead they show up like weak spectral lines.
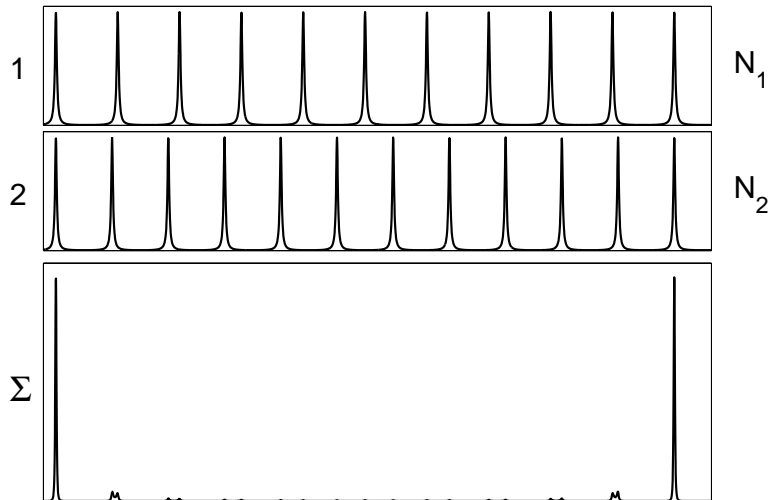
Figure 15: Interferogram of a monochromatic spectral line measured by a tandem interferometer. 1: interference order $N_1 = 1000$, 2: $N_2 = 1100$, $\sum$: combination of the two interferometers.
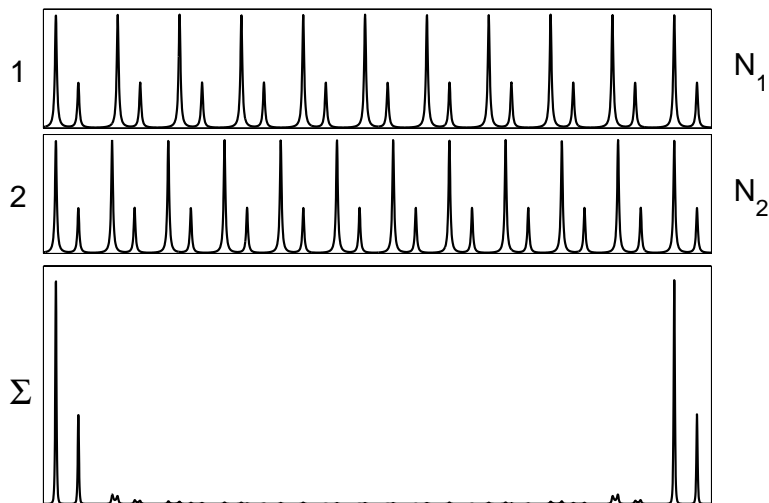

Figure 16: Interferogram of two adjacent monochromatic spectral lines measured by a tandem interferometer. 1: interference order $N_1 = 1000$, 2: $N_2 = 1100$, $\sum$: combination of the two interferometers.

To suppress these neighboring orders better, the tandem principle has to be combined with the multipass technique. The resulting effect is shown in Fig. 17. []
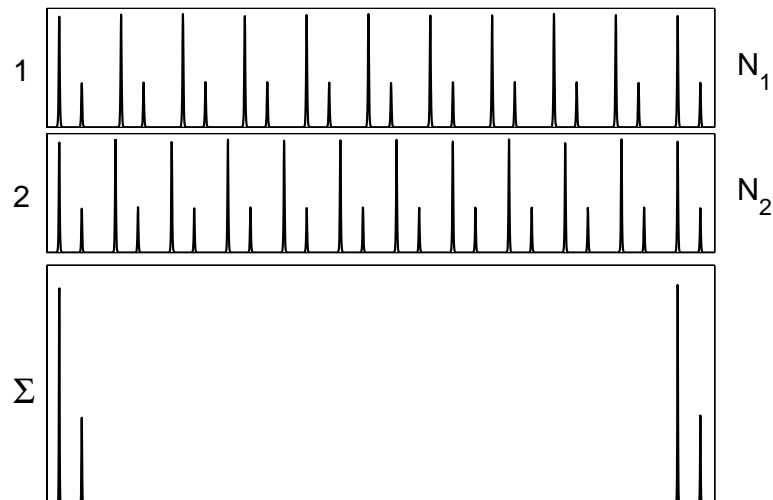
Figure 17: Effect of the combination of a tandem interferometer with the multipass technique (triple pass). 1 and 2: single interferometers in triple pass, $\sum$: combination of tandem and triple pass.

References

[1] Max Born, Emil Wolf. *Principles of Optics*. Pergamon Press, Oxford, fifth edition, 1975.

[2] J. R. Sandercock. *Simple stabilization scheme for maintenance of alignment in a scanning Fabry-Perot interferometer*. J. Phys. E **9**, 566 (1976).

[3] J. R. Sandercock. U. S. Patent , 4,014,614 (1977).

[4] J. R. Sandercock. U. S. Patent , 4,225,236 (1980).

[5] P. Jaquinot. *New Developments in Interference Spectroscopy*. Rep. Prog. Phys **23**, 268 (1960).